Stratospheric water vapour and ozone response to different QBO disruption events in 2016 and 2020

Mohamadou A. Diallo[1], Felix Ploeger[1, 2], Michaela I. Hegglin[1, 2, 3], Manfred Ern[1], Jens-Uwe Grooß[1], Sergey Khaykin[4], and Martin Riese[1, 2]

[1]Institute of Energy and Climate Research, Stratosphere (IEK–7), Forschungszentrum Jülich, 52 425 Jülich, Germany.
[2]Institute for Atmospheric and Environmental Research, University of Wuppertal, Wuppertal, Germany.
[3]Department of Meteorology, University of Reading, Reading, UK.
[4]Laboratoire Atmosphères, Milieux, Observations Spatiales, UMR CNRS 8190, IPSL, Sorbonne Univ./UVSQ, Guyancourt, France.

Correspondence: Mohamadou A. Diallo (m.diallo@fz-juelich.de)

Abstract. The Quasi-Biennial Oscillation (QBO) is a major mode of climate variability in the tropical stratosphere with quasi–periodically descending westerly and easterly winds, modulating transport and distributions of key greenhouse gases such as water vapour and ozone. In 2016 and 2020, anomalous QBO easterlies disrupted the QBO's mean period of about 28–months ~~QBO's 28–month period~~ previously observed. Here, we quantify the impact of these two QBO disruption events on the Brewer–Dobson circulation and respective distributions of water vapour ~~vapor~~ and ozone using the ERA5 reanalysis and the Microwave Limb Sounder (MLS) satellite observations, respectively. In 2016, both, water vapour and ozone in the lower stratosphere ~~Both lower stratospheric trace gases~~ decrease globally during the QBO disruption event by up to about 20 %. In 2020, the lower stratospheric ozone only weakly decreases during the QBO disruption event by up to about 10 %, while the lower stratospheric water vapour increases by up to about 15 %. These dissimilarities in the anomalous circulation and the related ozone response ~~circulation anomalous response~~ between the year 2016 and the year 2020 result from differences in the tropical upwelling and in the secondary circulation of the QBO caused by differences in anomalous planetary and gravity wave breaking in the lower stratosphere near the equatorward upper flanks of the subtropical jet. The anomalous of planetary and gravity wave breaking was stronger in the lower stratosphere between the tropopause and the altitude of about 23 km during the QBO disruption events in 2016 than in 2020. However, the differences in the response of lower stratospheric water vapour to the QBO disruption events between the year 2016 and the year 2020 are mainly due to the differences in cold–point temperatures induced by the Australian wildfire, which moistened the lower stratosphere, therefore, obscuring ~~hidding~~ the impact of the QBO disruption event in 2020 on water vapour in the lower stratosphere. Our results highlight the need for a better understanding of the causes of the QBO disruption, their interplay with other modes of climate variability in the Indo-Pacific region, including the El Niño Southern Oscillation (ENSO) and the Indian Ocean Dipole (IOD), and their impacts on water vapour and ozone in the upper troposphere/lower stratosphere in the face of a changing climate.

1 Introduction

The upper troposphere and lower stratosphere (UTLS) is a key region of the Earth climate system because of a large sensitivity of radiative forcing to greenhouse gas variations in that region, such as water vapour (H_2O) and ozone (O_3) (**???**). The transport and distribution of these trace gases in the UTLS is determined by the stratospheric Brewer-Dobson circulation (BDC), defined as the meridional overturning circulation which transports air masses upward from the tropics, poleward and then downward in the extratropics through its transition and shallow branches in the UTLS and its deep branch in the middle and upper stratosphere (**???**). Any changes in the composition of these radiatively active trace gases in the UTLS region induced by the BDC and its modulation by the modes of climate variability lead to large impacts on surface climate (e.g., **?????????**).

Ozone is mainly produced in the lower and middle stratosphere between about 16 km and 35 km altitude often referred to as the ozone layer (**???**). ~~Ozone is mainly produced in the middle stratosphere and is a good proxy of the tropical upwelling~~. In addition, ozone variability in the tropical lower stratosphere is a good proxy of the tropical upwelling of the BDC (**???**). The ozone transport and lifetime in the UTLS region are both modulated by the seasonality in the BDC and the modes of climate variability, such as the Quasi-Biennial Oscillation (QBO) ~~natural modes of climate variability, including the Quasi-Biennial Oscillation (QBO)~~ (**??**). Lower stratospheric water vapour and its multi-timescale variations ranging from day to decades are mainly controlled by changes in the tropical cold–point temperatures and its modulations by the natural climate variability ~~natural modes of climate variability, including the QBO~~ (**?????**). Therefore, the amount of water vapour in the UTLS region is directly linked to the dehydration (i.e. the process of removing water) of the air parcels crossing through the coldest temperatures in the tropical tropopause layer (e.g., between 14 and 19 km; **?**).

Mostly driven by gravity waves and equatorially trapped waves, the QBO is a quasi-periodic oscillation between tropical westerly and easterly zonal wind ~~shears~~ (**??**). The QBO is considered as a dominant mode of climate variability of the equatorial stratosphere and it globally impacts the transport and distributions of stratospheric trace gases, including water vapour and ozone. Both alternating QBO easterly and westerly zonal wind regimes ~~phases~~ modulate the vertical and meridional components of the BDC and affect temperature structure, therefore, impacting the water vapour and ozone composition and radiative feedback in the UTLS region (**???**).

The quasi-periodic QBO cycle of about 28–29 month period~~28–month period~~, which alternates between westerly and easterly zonal wind ~~shears~~, was subject to two disruptions in the past five years. In February 2016 and January 2020, the ~~anomalous~~ QBO westerlies in the tropical lower stratosphere were unexpectedly interrupted by anomalous QBO easterlies caused by planetary waves propagating from the mid-latitudes toward the equatorial region combined with equatorial convective gravity waves (**????**). Hitherto, there is no clear understanding of how these QBO disruption events are linked to anomalously warm or cold sea surface temperatures (**????**), volcanic aerosols (**??**), wildfire smoke (**???**) and climate change (**?**). However, recent study based on climate model simulations from phase six of the Coupled Model Intercomparison Project (CMIP6) predicts increased disruption frequencies to the quasi-regular QBO cycle in a changing climate (**?**). Previous studies also suggest that the QBO amplitude in the tropical stratosphere is decreasing in the lower stratosphere due to the climate change–induced strengthening of the tropical upwelling (**???**). Thus, in the context of a changing climate, the predictable QBO signal associated with the quasi-regular phase progression and amplitude as well as its potential impacts on UTLS composition faces an uncertain future. Therefore, it is of particular importance to quantify and better understand the different anomalous circulations and the impacts

of the QBO disruption events on UTLS water vapour and ozone, which have the potential to locally and globally affect the radiative forcing of the Earth's climate system through their impacts on surface temperatures (**????**).

~~Here, we quantify the similarity and differences in the strength and depth between the 2015–2016 and 2019–2020 disrupted QBO impacts on lower stratospheric water vapour and ozone from satellite observations.~~ Here we use satellite observations to quantify the similarities and differences in the strength and depth of perturbed/disrupted QBO impact in 2016 and 2020 on water vapour and ozone in the lower stratosphere. Also, we analyse the main drivers of the differences in anomalous circulation and UTLS composition changes. Section 2 describes the satellite observational data sets and the multivariate hybrid regression model used for the quantification. Section 3 describes the anomalous BDC and UTLS composition changes following the 2016 and 2020 QBO disruption events. Section 4 discusses the results of a well-established multivariate hybrid regression analysis to provide evidence for the impact of the QBO disruption events on lower stratospheric water vapour and ozone. Finally, we discuss the main reasons for the differences between the 2016 and 2020 impact of the QBO disruption events on BDC and UTLS composition, and the related dynamical processes associated with planetary and gravity wave dissipation, which are likely caused by the anomalous surface conditions associated with the strong El Niño Southern Oscillation (ENSO) in 2015–2016 and the strong Indian Ocean Dipole (IOD) in 2019–2020. We also discuss the differences in BDC and UTLS composition between 2016 and 2020 in terms of the particularly warm stratosphere in the context of Australian wildfire smoke in 2020. ~~Finally, we discuss the main reasons of the anomalous BDC and UTLS composition differences between the 2015–2016 and 2019–2020 disrupted QBO impacts in relationship to planetary and gravity wave dissipation likely caused by the anomalous surface conditions associated with the strong El Niño Southern Oscillation (ENSO) in 2015–2016, the strong Indian Ocean Dipole (IOD) in 2019–2020. We further discuss the differences between 2016 and 2020 in view of the particularly warmer stratosphere linked to Australian wildfire smoke in 2020.~~

2 Data and methodology

To quantify the QBO and Australian wildfire smoke impacts, we used the monthly mean, zonal mean ozone and water vapour mixing ratios from the Aura Microwave Limb Sounder (MLS) satellite observations covering the 2005–2020 period (**?**). The version 4.4 MLS data set used here has a vertical resolution of 2.5–3.5 km ranging from 8 to 35 km and 60 °S to 60 °N. The individual profile measurements of this version 4.4 have a precision and systematic uncertainty of about ±10–40 % and ±10–25 % for H_2O and ±0.02–0.04 ppmv and ±0.02–0.05 ppmv + ±5–10 % for O_3, respectively, with a spatial representativeness of ∼ 200–300 km along the orbital-track line of sight (**???**). Previous findings show that MLS monthly mean, zonal mean H_2O mixing ratios show very good agreement with 13 water vapour products from 11 limb-viewing satellite instruments, throughout most of the atmosphere (including the UTLS) with mean deviations from the multi-instrument mean between +2.5 % and +5 %, making these random errors irrelevant for the averaged monthly mean, zonal mean H_2O anomalies used in this study (e.g., **??**).

In addition to the MLS observation data sets, we also utilize the temperature (T) and zonal mean wind (U) for the 2005–2020 time period from the ERA5 reanalysis of the European Centre for Medium-Range Weather Forecasts (ECMWF) (**?**). We have

also calculated the residual circulation vertical velocity ($\overline{w^*}$) using the Transformed Eulerian Mean (TEM; **?**) and decomposed the wave drag into planetary wave dag (PWD) and gravity wave drag (GWD) contributions to the circulation anomalies (**??**). Note that we are using the ERA5 reanalysis data on the original 137 model levels for calculating the TEM budget, but not the coarse conventional pressure-level data, which can cause large uncertainties in the equatorial waves and zonal wind in the tropical stratosphere (**???**). For more details about the ERA5 TEM calculations and wave decomposition please see **?**.

We disentangle the QBO impact on the MLS monthly ~~these monthly~~ mean zonal mean stratospheric water vapour and ozone mixing ratios from the other sources of natural climate variability using a multivariate hybrid regression model for the 2005–2020 period (Eq. 1). In the figures, only the 2013–2020 period is shown to highlight the impact of the two QBO disruption events. ~~To highlight the two QBO disruptions, figures only show the 2013–2020 period~~. The established multivariate hybrid regression method is appropriate to separate the relative influences of the considered modes of climate variability, including the QBO, on stratospheric water vapour and ozone. Additional details about the multvariate hybrid regression model and its applications can be found in **?**. Our multvariate hybrid regression model decomposes the given monthly zonal mean variable, Var_i, into a long-term linear trend, seasonal cycle, modes of climate variability and a residual (ε). For a given variable Var_i (herein H_2O, O_3, $\overline{w^*}$, T, PWD and GWD), the multivariate hybrid regression model yields

$$Var_i(t_{month}, y_{lat}, z_{alt}) = Trend(t_{month}, y_{lat}, z_{alt}) + SeasCyc(t_{month}, y_{lat}, z_{alt}) + \sum_{n=1}^{5} b_n(y_{lat}, z_{alt}) \cdot Proxy_n(t_{month} - \tau_n(y_{lat}, z_{alt})) + \varepsilon(t_{month}, y_{lat}, z_{alt}), \quad (1)$$

where $Proxy_n$ represents the different climate indices ~~indexes~~ used here. $Proxy_1$ is a normalized QBO index (QBOi) from the 5°S–5°N ERA5 zonally averaged zonal mean winds with full vertical levels then deseasonalised and normalized by the standard deviation to build the QBOi (**?**). $Proxy_2$ is the normalized Multivariate ENSO Index (MEI; **?**), $Proxy_3$ is the Indian Ocean Dipole (IOD, **?**), $Proxy_4$ is the Madden-Julian Oscillation (MJO, **?**), and $Proxy_5$ is the Aerosol Optical Depth (AOD) from satellite data (**??**). $Trend(t_{month}, y_{lat}, z_{alt})$ is a linear trend. $SeasCyc(t_{month}, y_{lat}, z_{alt})$ is the annual cycle. The coefficients are the amplitude b_n and the lag $\tau_n(y_{lat}, z_{alt})$ associated with the QBO, ENSO, IOD, MJO and AOD respectively. The solar forcing is neglected because our data set is relatively short. Finally, we estimate the uncertainty in the multivariate hybrid regression model using a Student's t test technique (**??**).

3 Characterisation of the 2016 and 2020 anomalous circulations

~~In~~ In February 2016 and January 2020 unexpected tropical QBO easterlies (negative QBOi) developed ~~the center of~~ into the downward propagating tropical QBO westerlies between the altitude of 16 km and 25 km, thereby breaking the quasi-regular QBO cycle of alternating easterly and westerly phases (Fig. 1a and Fig. S1a, b in the supplement) (**???**). Both QBO disruption events have been associated with a combination of extratropical Rossby waves, equatorial planetary waves (Kelvin, Rossby, mixed Rossby–gravity, and inertia–gravity), and small–scale convective gravity waves, propagating into the deep tropics and depositing their negative momentum forcing (**????**). Both QBO disruption events were~~are~~ primarily triggered by mid-latitude

Rossby waves propagating from the northern hemisphere in 2016 and from the southern hemisphere in 2020 into the deep tropical lower stratosphere. In 2016, the equatorial planetary wave forcing may have preconditioned mid-latitude Rossby waves to break easily at the equator (e.g., **?**), while in 2020, the equatorial planetary and small-scale convective gravity waves propagating into the UTLS predominantly contributed to the disruption (**??**). Note that the potential processes and mechanisms triggering the QBO disruption are still under debate. Recent findings from **?** using a 1D theorical model of the QBO from **?** pointed out the key role of the upwelling and wave dissipation. Details regarding the triggering of QBO disruptions has been the focus of several recent studies (e.g. **?????????**). Although similar in many respects, including the causes of the sudden development of tropical QBO easterlies ~~the center~~ into of tropical QBO westerlies between the altitude of 16 km and 25 km, the two QBO disruption events also exhibit differences, particularly in the structure (strength and depth) of their impacts and the level at which the shift started (Fig. 1a). Here, we mainly focus on the impact of the QBO disruption events on the lower stratospheric BDC and on the distributions of trace gases like water vapour~~vapor~~ and ozone.

The similarities as well as the differences between the two disruption events are also visible in the inter-annual variability of the tropical lower stratospheric zonal mean zonal wind (a), H_2O (b) and O_3 (c) anomalies as a percentage change relative to the monthly mean mixing ratio during the 2013–2020 period (Fig. 1a–c). Both QBO disruption events are expected to impact the tropical upwelling of the BDC through the two way interactions between the mean–flow and wave propagation associated with the QBO phases (**???????**) as well as through its control of the tropical cold–point temperatures (**??**). ~~This impact of the QBO disruption events in 2016 and 2020 on the transport and distribution of lower stratospheric H_2O and O_3 mixing ratios are most effective when the signal reaches the tropical cold–point tropopause (∼17 km), e.g. from June to December in 2016 and from June to August in 2020 (Fig. 1)~~ The impacts of the QBO disruption events in 2016 and in 2020 on the transport and distribution of lower stratospheric H_2O and O_3 mixing ratios is most effective when the anomalous QBO easterlies reach the tropical cold–point temperature altitude (∼17 km) with associated enhanced tropical upwelling both driven by the anomalous wave breaking from June to December in 2016 and from June to August in 2020 (Fig. 1) (**??**). The zonal mean, zonal wind shows that the westerly jet between the onset and offset time period and at the altitude of 25 km is stronger and deeper during the QBO disruption event in 2016 than during the QBO disruption event in 2020 (Fig. 1a and Fig. S1c, d in the supplement). The QBO disruption event in 2020 shows a clear separation of the westerlies into two parts while the QBO disruption event in 2016 reestablishes the westerlies at the top of the easterlies, e.g. at the altitude of about 25 km (Fig. 1a). As soon as the downward propagation of tropical QBO easterlies reaches the tropical cold–point temperature altitude (∼17 km) from June to December 2016, the H_2O mixing ratios decrease i.e. turning from positive to negative anomalies. As reported by **?**, the alignment of the strong El Niño event with westerly QBO in early boreal winter of 2015–2016 (September 2015–March 2016) substantially increased H_2O mixing ratios and decreased O_3 mixing ratios by up to about 20 % in the tropical lower stratosphere between the tropopause (∼16 km) and the altitude of about 23 km (Fig. 1b–d). The sudden occurrence of the QBO disruption event decreased the lower stratospheric H_2O and O_3 mixing ratios from late spring to early following winter by up to about 20 % (Fig. 1b–d).

Conversely during the QBO disruption event in 2020, Figure 1b–d show clear differences in the tropical lower stratospheric trace gas anomalies, particularly in the strength and depth of H_2O and O_3 anomalies, consistent with the structural zonal mean

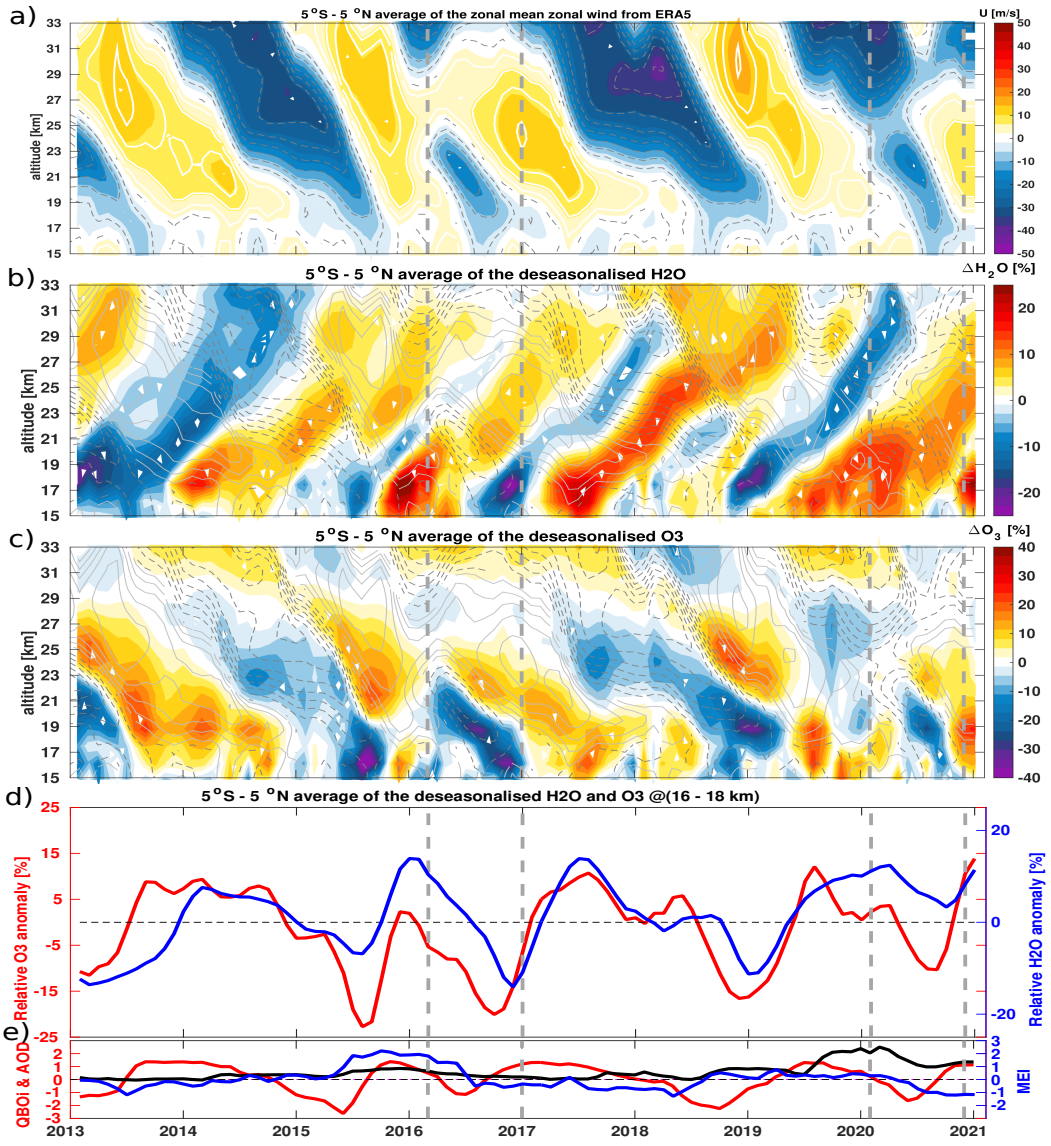

Figure 1. Tropical average of the zonal mean zonal wind (U) from the ERA5 reanalysis and deseasonalized stratospheric H_2O and O_3 time series from MLS satellite observations for the 2013–2020 period in percent change from long-term monthly means as a function of time and altitude. Shown are **(a)** Zonal mean zonal wind U, **(b)** Deseasonalized monthly mean H_2O anomalies, **(c)** Deseasonalized monthly mean O_3 anomalies. **(d)** Tropical average of the deseasonalized lower stratospheric H_2O (blue) and O_3 (red) time series between the altitude of 16 and 18 km. The lowermost panel **(e)** shows the QBO index at 50 hPa (21 km) in red, the MEI index in blue and the AOD index in black. The vertical grey dashed lines indicate February 2016 and January 2020 for the QBO disruption onset and December 2016 and November 2020 for the QBO disruption offset. Monthly averaged zonal mean zonal wind component, U ($m\,s^{-1}$), from the ERA5 reanalysis, is overlaid as solid white (westerly wind) and dashed grey (easterly wind) contour lines.

zonal wind changes (Fig. S1c, d). The tropical lower stratospheric O_3 anomalies are purely responding to the enhanced tropical upwelling of the BDC caused in 2016 by a combination of a strong El Niño event, negative IOD event and the QBO disruption event in 2016, and in 2020 by a combination of a weak La Niña, strong positive IOD event and the QBO disruption events in 2020 (e.g., easterly winds between 16 km to 23 km (100–40 hPa)) (**?**). Tropical lower stratospheric O_3 anomaly is a good proxy of the tropical upwelling of the BDC as its concentration is modulated by the advection of tropospheric air generally poor in O_3 into the stratosphere (**?????**). The small decrease in the tropical lower stratospheric O_3 anomalies by up to about 10 % in 2020 compared to about 20 % in 2016 between the altitude of 16 km and 23 km suggests a stronger tropical upwelling and its modulations in 2016 than in 2020 (Fig. 1c, d).

The inter-annual variability in large-scale upward advection of the tropical stratospheric H_2O anomalies (i.e. tape recorder) is more challenging to interpret because of its regulation by the variability in the tropical cold–point temperatures (**????**). The negative tropical lower stratospheric H_2O anomalies induced by the interplay of different modes of natural climate variability, including the QBO, are weaker in 2020 than in 2016 (Fig. 1b, d and Fig. S2a, b in the supplement). The tropical lower stratospheric H_2O anomalies averaged between the altitude of 16 km and 18 km are up to about 20 % more negative in 2016 than in 2020 (Fig. 1b, d and Fig. S2a, b in the supplement). Particularly, the 2020 tape recorder shows positive H_2O anomalies as large as 15 % even after the QBO disruption event that are of opposite sign to the 2016 H_2O anomalies (Fig. 1b, d). This complexity in H_2O inter-annual variability lies in its dependency on the interplay of different modes of climate variability, including the QBO (**????**), volcanic aerosols (**?????**), seasons (early or late in the winter) and location (western, central or eastern Pacific, where the ENSO and IOD maximum occurs (**??**)). Therefore, to elucidate the impact of the two QBO disruption events on the Brewer–Dobson circulation and respective distributions of lower stratospheric H_2O and O_3 anomalies, we performed a regression analysis both without and with explicitly including QBO signals to isolate the QBO impact on these trace gases. The difference between the residual (ε in Eq. 1) with and without explicit inclusion of the QBO signals provides the QBO–induced impact on stratospheric H_2O and O_3 anomalies. Also, the impact of 2020 Australian wildfire smoke on stratospheric H_2O anomalies is analogously obtained by differencing the residuals of the regression model. This approach of differencing the residuals is similar to direct calculations, projecting the best fits of the regression onto the QBO basis functions, i.e., the QBO predictor timeseries (see supplement Figs. 2 and 4 in **?**). In addition, this differencing approach avoids the need to reconstruct the time series after the regression analysis.

4 Drivers detection and attribution of the anomalous circulations

4.1 Impact of QBO disruptions on UTLS composition

Figures 2a, b show time series of the QBO–induced inter-annual variability in tropical lower stratospheric H_2O and O_3 anomalies estimated from the difference between the residual (ε in Eq. 1) without and with explicit inclusion of the QBO proxy for the 2013–2020 period. A footprint of both QBO disruption events is clearly visible in lower stratospheric H_2O and O_3 anomalies with a shift from positive anomalies related to the westerly winds (positive QBOi) to negative anomalies related to the easterly winds (negative QBOi). The impacts of the QBO disruption events on lower stratospheric O_3 anomalies ~~sudden and~~ clearly

follow the monthly mean zonal mean wind changes. The impact of the QBO disruption event on lower stratospheric H_2O anomalies are delayed by about 3–6 months compared to the zonal wind anomalies because of the H_2O tropospheric origin as well as its dependency on the tropical cold–point temperature anomalies. ~~The QBO disruption–induced H_2O anomalies are barely in phase with the zonal wind anomalies with a delay of about 3–6 months because of the H_2O tropospheric origin as well as its dependency on the tropical cold–point temperature anomalies.~~

Beside the good agreement in the structure of both trace gas changes, there are clear differences in the strength and depth of both lower stratospheric H_2O and O_3 responses to the QBO disruptions between the 2016 and the 2020 events and, particularly large for the H_2O response. These differences in the impact of the QBO disruption events are consistent with the observed lower stratospheric H_2O and O_3 anomalies (Fig. 1, Fig. 2 and Fig. S2). During 2016, the QBO shift from westerlies to easterlies at the altitude of about 23 km (40 hPa) in the tropical lower stratosphere induces substantial negative H_2O and O_3 anomalies of up to about 20 % between the altitude of 16 km and 23 km from the early boreal summer to the next boreal winter for H_2O and from the early boreal spring to the next boreal winter for O_3 (Fig. 2). This decrease in H_2O and O_3 mixing ratios is consistent with upward transport of young and dehydrated air as well as poor in O_3 into the lower stratosphere between the altitude of 16 km and 23 km. As expected, the sudden occurrence of the QBO disruption events caused anomalously low cold–point temperatures and enhanced tropical upwelling in 2016 and in 2020, consistent with the decrease in H_2O and O_3 mixing ratios induced by the QBO easterly (Fig. 2). However, besides the similarities in the structural changes, the negative H_2O and O_3 anomalies induced by the QBO disruption are smaller and shallower in 2020 than in 2016. While differences between the 2016 and 2020 impact of the QBO disruption events on O_3 are small, the differences between the 2016 and 2020 O_3 anomalies are particularly large due to other modes of natural variability (Fig. 1c, d and Fig. 2b, d). ~~While the differences in the O_3 anomalies induced by the QBO disrution events are small between the year 2016 and year 2020, the differences in the disrupted QBO impact on O_3 mixing ratios are particularly large between the year 2016 and year 2020 (Fig. 2b, d).~~ The differences in the magnitude of negative O_3 anomalies suggest a weaker modulation of the anomalous tropical upwelling of the BDC by the secondary circulation in 2020 than in 2016, consistent with the differences in the strength and depth of the residual vertical velocity and wave forcing anomalies discussed in Sect. 4.2. The differences in the strength and depth of the H_2O response to the QBO disruption events suggest that the tropical cold–point temperature is substantially different between the year 2016 and year 2020. In addition, we note that the ~~early~~ QBO westerly followed by the shift to QBO easterly is not the main cause of the large increase in the 2020 lower stratospheric H_2O anomalies. In the following, we assess the potential impact of the unusually strong Australian wildfire smoke on the lower stratospheric H_2O anomalies in 2020 through its impact on the stratospheric temperature anomaly (**???**).

Figures 3a–d show the impact of the QBO disruption events on the zonal mean lower stratospheric H_2O and O_3 anomalies estimated from the difference between the residual (ε in Eq. 1) without and with explicit inclusion of the QBO signal for the 2005–2020 time period. Figure 3e shows the impact of the 2020 Australian wildfire on lower stratospheric H_2O anomalies estimated from the difference between the residual (ε in Eq. 1) without and with explicit inclusion of the AOD signal for the 2005–2020 time period. The lower stratospheric H_2O anomalies are averaged from July to December for 2016 and from July to September for 2020 respectively. We chose different averaging periods for 2016 (July–to–December) and 2020 (July–August–

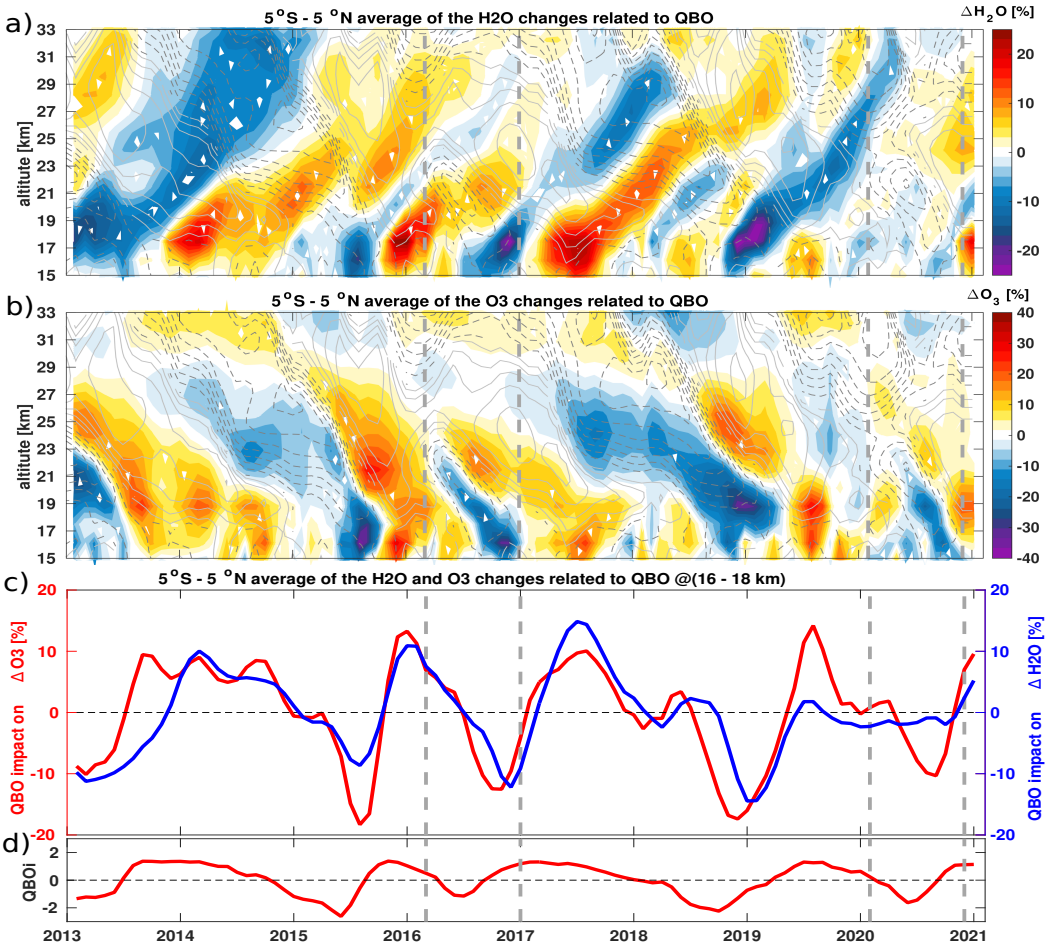

Figure 2. QBO impact on the tropical average of the stratospheric H_2O **(a)** and O_3 **(b)** anomalies from the MLS satellite observations for the 2013–2020 period in percent change relative to monthly mean mixing ratios as a function of time and altitude. **(c)** QBO impact on tropical average of the lower stratospheric H_2O (blue) and O_3 (red) time series between the altitudes of 16 and 18 km. Shown QBO impact on the stratospheric trace gases is derived from the multiple regression fit as the difference between the residual (ε in Eq. 1) without and with explicit inclusion of the QBO signal. The lower panel **(d)** below indicates the QBO index at 50 hPa (21 km) in red. The vertical grey dashed lines indicate February 2016 and January 2020 for the QBO disruption onset and December 2016 and November 2020 for the QBO disruption offset. Monthly averaged zonal mean zonal wind component, U ($m\,s^{-1}$), from the ERA5 reanalysis, is overlaid as solid grey contours (westerly) and dashed grey contours (easterly) lines.

September) to have similar zonal mean structure of the H_2O and O_3 ~~anomalies~~ response to QBO disruption events, although their depth and strength are different from each other.

225 In 2016, the shift to QBO easterly phase in the tropics significantly dehydrates the global lower stratosphere by up to about 20 % below the altitude of 18 km (Fig. 3a and Fig. 1b) (**??**). This decrease in H_2O mixing ratios is due to the enhanced tropical

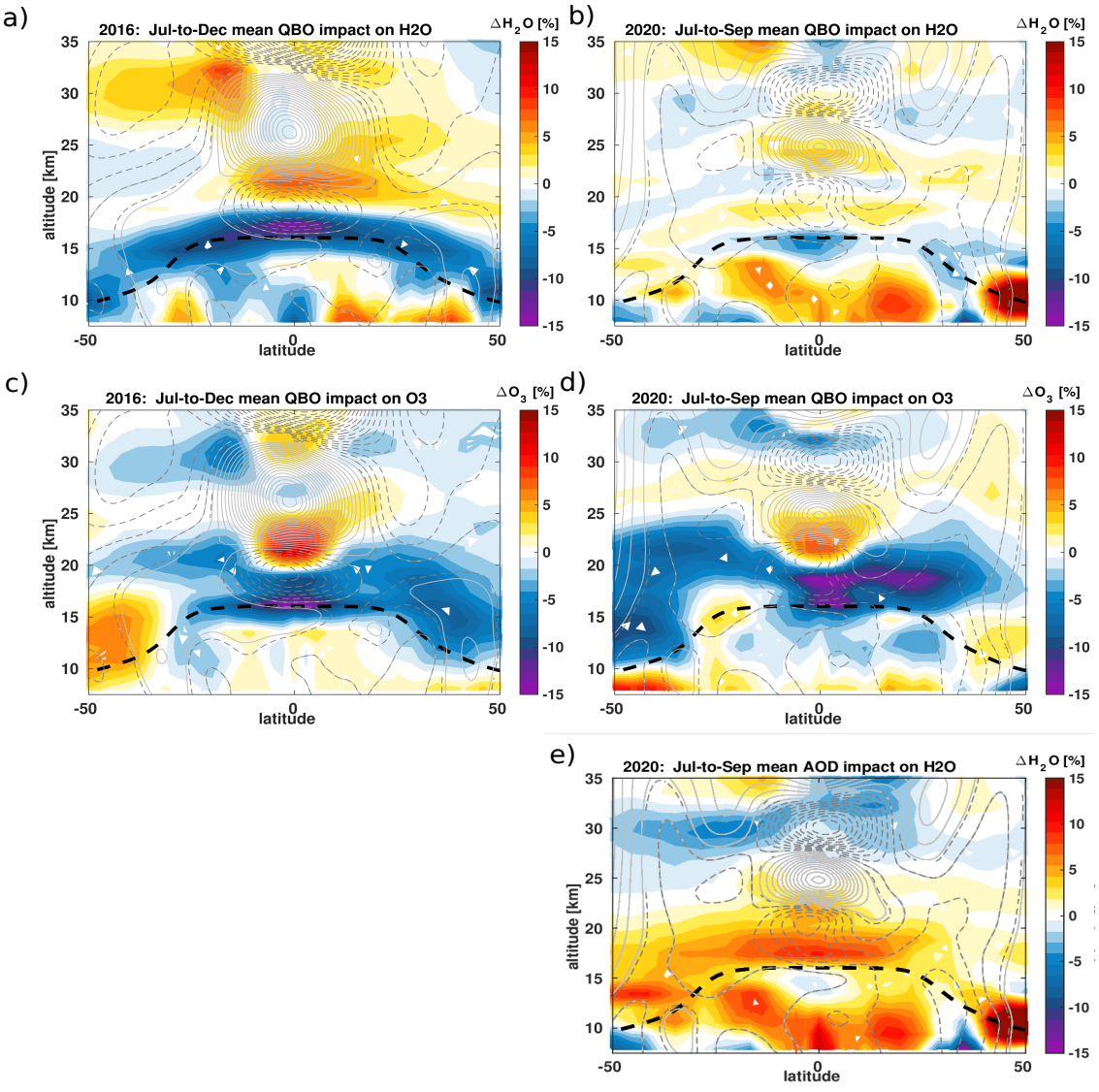

Figure 3. Impact of the QBO disruption on the zonal mean lower stratospheric H_2O **(a, b)** and O_3 **(c, d)** anomalies from MLS satellite observations averaged from July to December for 2016 **(a, c)** and from July to September for 2020 **(b, d)** period. In addition, the impact of the 2020 Australian wildfires on the zonal mean lower stratospheric H_2O is shown **(e)**. All panels show the percentage change relative to 2005–2014 monthly mean mixing ratios as a function of latitude and altitude. The impact of the QBO disruptions and the Australian wildfire on the stratospheric trace gases is derived from the multiple regression fit as the difference between the residual (ε in Eq. 1) without and with explicit inclusion of the QBO signal. The black dashed horizontal line indicates the tropopause from the ERA5 reanalysis. Monthly averaged zonal mean zonal wind component, U ($m\,s^{-1}$), from the ERA5 reanalysis, is overlaid as solid grey (westerly wind) and dashed grey (easterly wind) contours lines.

upwelling of the BDC, its modulation by the secondary circulation of the QBO and the related decrease of tropical cold–point temperatures as discussed later in Sect. 4.2 (**?????**). Because of the hemispheric asymmetry of the BDC (e.g. stronger in the winter hemisphere) driven by planetary wave activity (e.g. **?**) and eddy mixing (e.g. **?**), the rising dehydrated air from the tropics moves toward middle and high latitudes of both hemispheres ~~stronger in winter hemisphere~~. The positive H_2O anomalies above the altitude of 18 km are related to the effect of the preceding QBO westerly phase on tropical UTLS temperatures and the upward propagating tape-recorder signal. The negative H_2O anomalies are consistent with the observed negative tropical O_3 anomalies below the altitude of 20 km induced by the QBO easterly phase (Fig. 3a, c and Fig. S2a, c in the supplement). These changes indicate an enhanced tropical upwelling of the BDC and its modulation by the QBO easterly phase in the lower stratosphere between the altitude of 16 km and 18 km. The positive tropical O_3 anomalies above the altitude of 20 km, are associated with the QBO westerly phase (Fig. 3c and Fig. S2c in the supplement). The large variability in extratropical O_3 anomalies shown in Figure 3c are related to the QBO influence on the extratropical circulation (**???**), stratospheric major warmings, and chemical processes (**?**).

In 2020, the impact of the QBO disruption event on the tropical lower stratospheric H_2O and O_3 anomalies exhibits a similar structure as the effect of the QBO disruption event in 2016. Note that we use different averaging periods for 2016 (July–to–December) and 2020 (July–to–September) to highlight the structural similarities in the QBO impact. Both trace gases show negative anomalies in the tropics, corroborating the enhanced tropical upwelling of the BDC induced by the QBO shift from westerly winds to easterly winds in the tropics (Fig. 3b). However, there are also differences in both lower stratospheric H_2O and O_3 responses to the shift from the tropical QBO westerly phase to the tropical QBO easterly phase between July–to–December 2016 and July–to–September 2020. Note that the differences in the impact of the QBO disruption events on H_2O between the year 2016 and the year 2020 are particularly large, up to about 20 % (Fig. 2a, c and 3a, b). Conversely to the globally dehydrated lower stratosphere in 2016, the sudden development of tropical QBO easterly winds in 2020 led to a small decrease in lower stratospheric H_2O mixing ratios, therefore, to small negative lower stratospheric H_2O anomalies up to about 2–3 % (Fig. 2c and Fig. 3b). Despite the similar zonal mean structure of O_3 anomalies induced by both QBO disruption events within these different averaging periods for 2016 (July–to–December) and 2020 (July–to–September), the impact of the QBO disruption events on the zonal mean O_3 mixing ratios are weaker when averaged in the entire year 2020 than in the year 2016 (Fig. 3c, d and Fig. S2c, d in the supplement). The differences in the strength and depth between the 2016 and 2020 H_2O and O_3 anomalies and their modulation by the QBO disruption events clearly suggest substantial differences in the anomalous tropical upwelling of the BDC and the tropical cold–point temperatures discussed in Sect. 4.2. The smaller negative tropical O_3 anomalies suggest that the tropical upwelling of the BDC and its modulation by the QBO–induced secondary circulation are weaker in 2020 than in 2016 (Fig. 3c, d). Simultaneously, the positive tropical H_2O anomalies in 2020 that are not related to the QBO disruption event indicate warmer tropical cold–point temperatures potentially induced by the unusually strong Australian wildfire smoke in the stratosphere (**???**). The main dynamical causes of these differences are investigated in the following section.

4.2 Mechanisms driving the strength and depth differences

To further investigate and understand the key drivers of the anomalous circulation differences between the 2016 and 2020 impact of the QBO disruption events, we analyse the differences in the tropical upwelling of the BDC and the secondary circulation induced by the QBO wind shear. Figure 4a–d show time series of the tropical residual circulation vertical velocity and temperature anomalies together with the impacts of the two QBO disruption events on $\overline{w^*}$ and temperature anomalies during the year 2016 and year 2020, respectively. Also, Figure 5a–h show latitude–altitude sections of the $\overline{w^*}$ and temperatures together with the associated impacts of the QBO disruption events during the year 2016 and the year 2020 periods.

Clearly, Figure 4 and 5 show that there are substantial differences in the anomalous tropical upwelling of the BDC as disclosed by $\overline{w^*}$ and temperature anomalies during the two disruption events, consistent with the O_3 anomalies (Fig. 1c, d). Also, the modulation of the tropical upwelling by the QBO disruption events exhibits differences but smaller than the net anomalous circulation differences during the two periods, consistent with the impact of the QBO disruption events on O_3 anomalies (Fig. 2b, c). In 2016, the tropical upwelling anomalies strongly increased up to about 45 % below the altitude of about 18 km from April to December when the QBO westerly phase shifts to QBO easterly phase (Fig. 4a). However in 2020, the tropical upwelling anomalies are weaker and only reach up to about 20 % below the altitude of about 18 km, leading to about 25 % weaker $\overline{w^*}$ anomalies in 2020 than in 2016 between the altitude of about 17 km and 20 km. At an altitude of about 17 km between the onsets and offsets, $\overline{w^*}$ anomalies were up to about 10–15 % weaker in 2020 than in 2016 (Fig. 4a). In addition to the weaker tropical upwelling in 2020, the impact of the QBO disruption events on $\overline{w^*}$ anomalies is consistent with the weaker QBO–induced secondary circulation in 2020 than in 2016 with up to about 25 % weaker modulation of the tropical upwelling (Fig. 4b). This weaker tropical upwelling of the BDC and the QBO–induced secondary circulation in 2020 than in 2016 is also visible in the zonal mean cross section of the mean $\overline{w^*}$ and temperature anomalies (Fig. 5a, b, e, f), together with the impacts of the QBO disruption events on $\overline{w^*}$ and temperature anomalies for 2016 and 2020 (Fig. 5c, d, g, h). The increase of the tropical upwelling as well as the secondary circulation associated to the QBO easterly wind shear between the tropopause height and altitude of about 18 km are weaker and shallower in 2020 than in 2016 (Fig. 4b and Fig. 5c, d). The differences in the anomalous tropical upwelling and secondary circulation are also consistent with the differences in the temperature anomalies as well as in the impact of the QBO disruption events on temperature anomalies (Fig. 4c, d and Fig. 5e–h). In 2016, the tropical temperature anomalies, in particular around the cold-point tropopause at about 17 km, are strongly negative (Fig. 4c). This decrease in tropical temperatures is consistent with the strong tropical upwelling of the BDC and its modulation by the QBO–induced secondary circulation (Fig. 4b, d and Fig. 5a, c, e, g), which, in turn led to large negative tropical lower stratosphere H_2O and O_3 anomalies in 2016.

Conversely, the tropical cold–point temperature anomalies are warmer and barely exceeding −0.1 K in 2020, consistent with the smaller tropical $\overline{w^*}$ anomalies (Fig. 4 and Fig. 5b, d, f, h) and the shorter lifetime of tropical O_3 anomalies, which last for only about 3 months (Fig. 1 and Fig. 2). These warmer tropical cold–point temperature anomalies corroborate the weaker tropical upwelling of the BDC and smaller tropical lower stratospheric H_2O and O_3 mixing ratios in the year 2020. Interestingly, the differences in the tropical cold–point temperature anomalies between the year 2016 and the year 2020 are

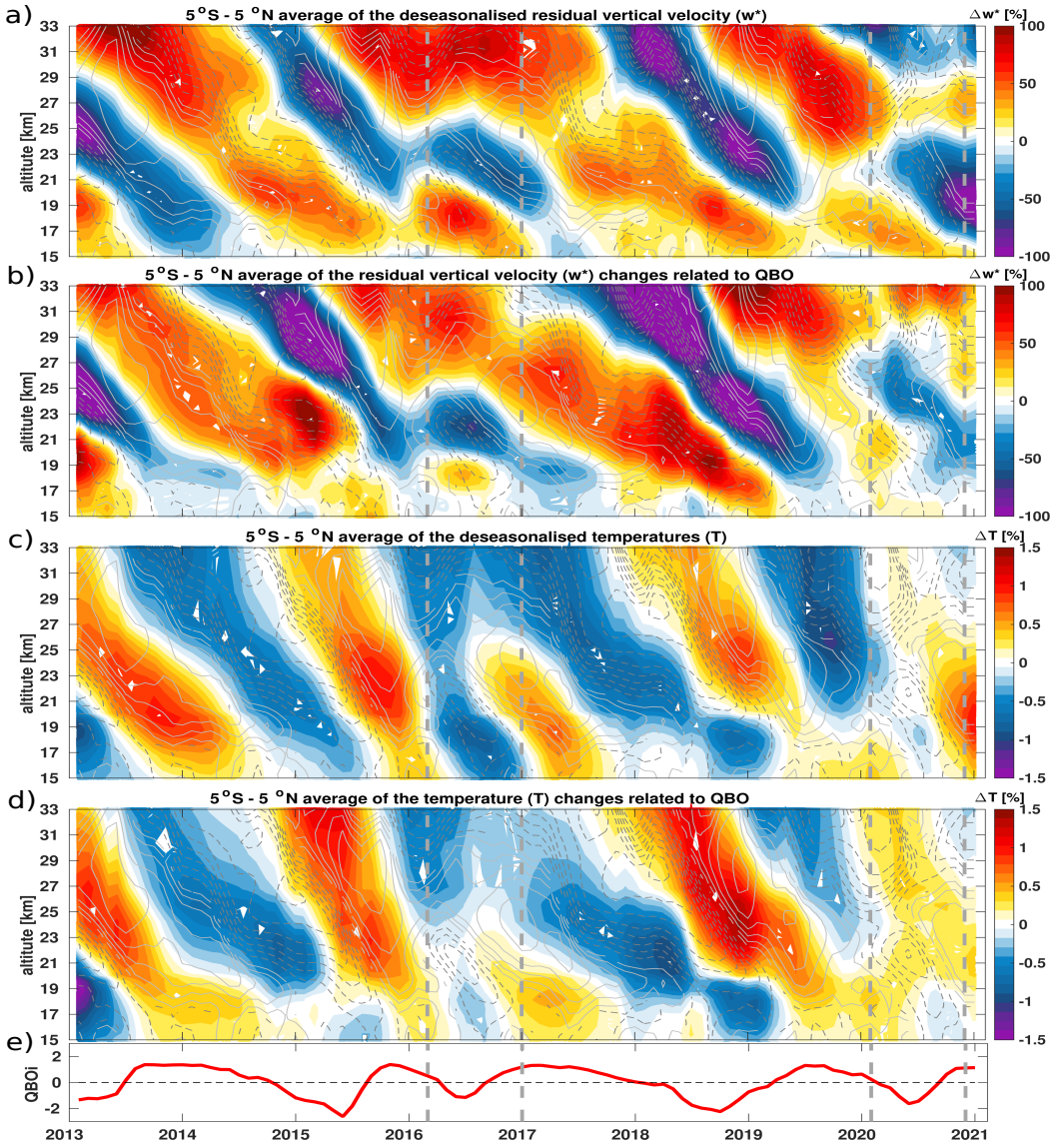

Figure 4. Tropical average of the deseasonalized mean residual vertical velocity ($\overline{w^*}$) and temperature anomalies time series the ERA5 reanalysis for the 2013–2020 period together with the impact of QBO disruptions on the tropical mean $\overline{w^*}$ and temperature anomalies derived from the multiple regression fit as a function of latitude and altitude. **(a)** Deseasonalized monthly mean tropical upwelling. **(b)** Disrupted QBO impact on monthly mean tropical upwelling anomalies. **(c)** Deseasonalized monthly mean tropical temperature. **(d)** Disrupted QBO impact on monthly mean tropical temperature anomalies. The vertical grey dashed lines indicate February 2016 and January 2020 for the QBO disruption onset and December 2016 and November 2020 for the QBO disruption offset. The lowermost panel **(e)** shows the QBO index at 50 hPa (21 km) in red. Monthly averaged zonal mean zonal wind component, U ($\mathrm{m\,s^{-1}}$), from the ERA5 reanalysis, is overlaid as solid grey (westerly) and dashed grey (easterly) contours lines.

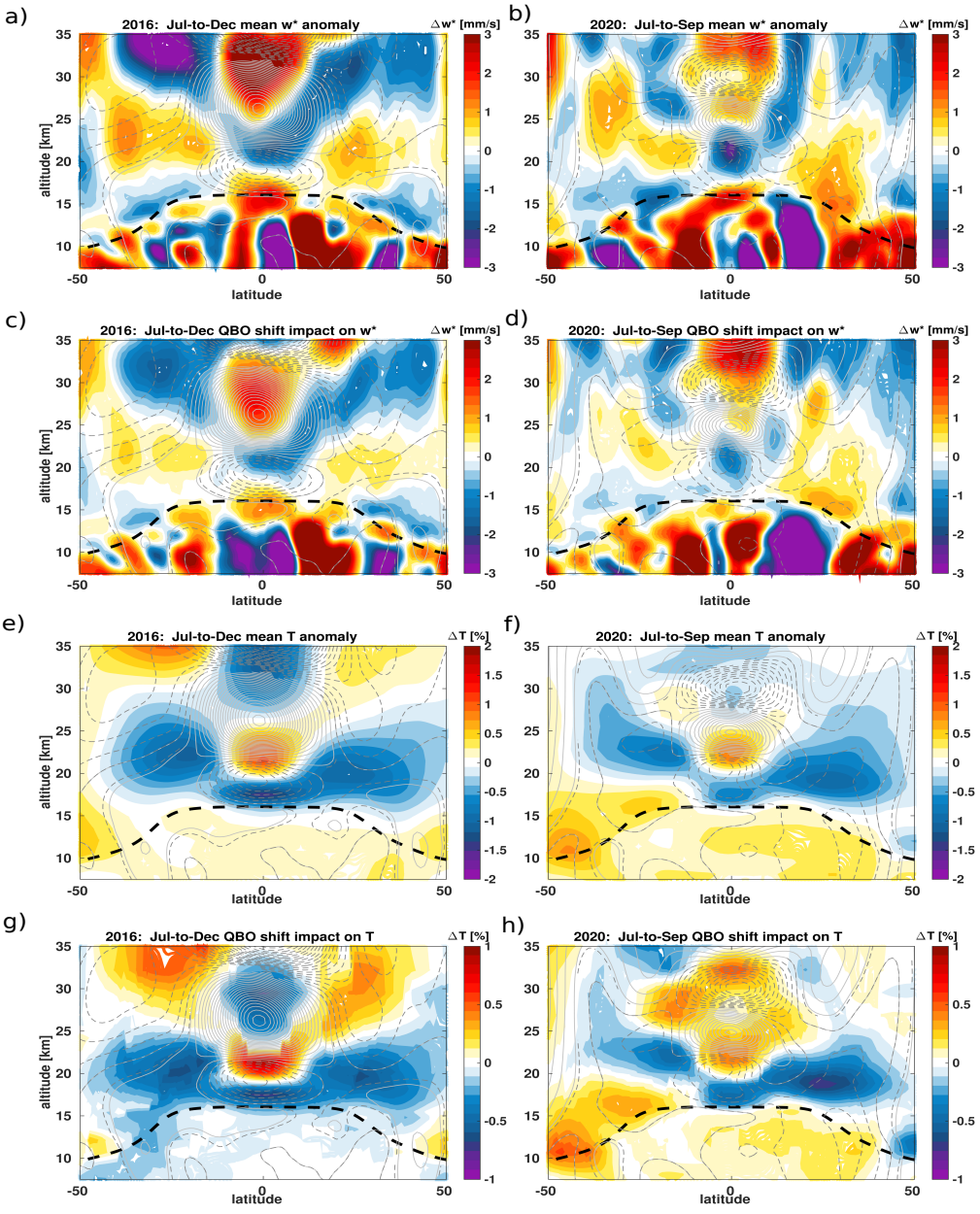

Figure 5. Zonal mean residual vertical velocity ($\overline{w^*}$) **(a, b)** and temperature anomalies **(e, f)** from the ERA5 reanalysis together with the impact of QBO disruption events on $\overline{w^*}$ **(c, d)** and temperature anomalies **(g, h)** derived from the multiple regression fit for the years 2016 **(a, c, e, g)** and 2020 **(b, d, f, h)**. The anomalies are as a deviation from the 2005–2014 zonal mean $\overline{w^*}$ and temperature. The black dashed horizontal line indicates the tropopause from the ERA5 reanalysis. Monthly mean zonal mean wind component, U ($\mathrm{m\,s^{-1}}$), from the ERA5 reanalysis is overlaid as solid grey contours (westerly) and dashed grey contours (easterly) lines.

more pronounced as shown in Figure 5e, f than the differences in the impact of the QBO disruption events on tropical cold–point temperature anomalies (Fig. 5g, h). This anomalously warmer stratosphere, including high cold–point temperatures in 2020, is consistent with recent findings about the impact of Australian wildfire smoke (**???**). Therefore, we also pay attention to volcanic eruptions and Australian wildfire smoke in 2020, which can impact lower stratospheric temperatures, and therefore, lower stratospheric H_2O and O_3 anomalies. Indeed using our regression analyses, we can show that the Australian wildfire largely moistened the lower stratosphere between the altitude of 16 km and 25 km in 2020 by inducing an anomalously warmer stratosphere, thereby, hiding the impact of the QBO disruption event in 2020 on H_2O anomalies (Fig. 3e). The removal of Australian wildfire impact allows to better highlight the weak structure of the impact of the QBO disruption event in 2020 on lower stratospheric H_2O anomalies between the altitude of 16 km and 25 km, which is similar to the impact of the QBO disruption event in 2016. Regarding the differences in the upwelling of the BDC, in the following, we finally investigate the related wave drag changes.

To investigate the main causes of the BDC differences between the year 2016 and the year 2020 during the QBO disruption events, we calculate the planetary and gravity wave drag as well as the net wave forcing. We analyse the differences in terms of wave activities potentially induced by specific sea surface conditions such as the unusually warm 2015–2016 El Niño and the 2019–2020 strong positive Indian Dipole Ocean, which impact tropical convective activities (**?**). For additional details about the wave decomposition please see **?** and **?**.

The BDC and its inter-annual variability are driven by the planetary and gravity wave breaking in different stratospheric regions (**?????**). Therefore, any changes in wave drag will lead to circulation and composition changes. Figure 6a–f show the January-to-June zonal mean of the deseasonalized monthly mean net wave forcing (NetF = PWD + GWD - du/dt), planetary wave drag (PWD) and gravity wave drag (GWD) from the ERA5 reanalysis for the years 2016 and 2020, respectively. Note that the net wave forcing is equal to the contribution of Coriolis force plus meridional advection plus vertical advection to the momentum balance (**?**). Clearly, the net wave forcing anomalies as well as the planetary and gravity wave drag anomalies exhibit differences in strength and depth in the lower stratosphere between the 2016 and 2020 QBO disruption events. During the QBO disruption event in 2016, the net wave breaking is stronger and broader in the lower stratosphere between the tropopause and the altitude of about 23 km than during the QBO disruption in 2020 (Fig 6a, b and Fig. S3a). Particularly, the wave breaking near the equatorward upper flanks of the subtropical jet (e.g. region between 30° S–10° S/10° N–30° N and above the tropopause level) known as a major BDC forcing region is weaker in 2020 than 2016 and this region is narrower (e.g. more tropically confined) in 2020. These differences in net wave forcing are the main cause of a weaker advective BDC and its modulation by the QBO–induced secondary circulation in 2020 than in 2016, therefore, contributing to the anomalous lower stratospheric H_2O and O_3 differences in addition to the significant Australian wildfire effect on lower stratospheric H_2O mixing ratios. ~~The time variation of wave forcing during six months (January–to–June) after the QBO disruption events is consistent with the zonal mean differences in wave forcings, i.e. the time series of net forcing, planetary and gravity wave drag (Fig. S3a–c).~~

In addition, we show the contribution of planetary (Fig. 6c, d, and Fig. S3b) and gravity (Fig 6e, f and Fig. S3c) wave drag to better understand the role of each forcing in the circulation anomalies differences during both QBO disruption events. Beside

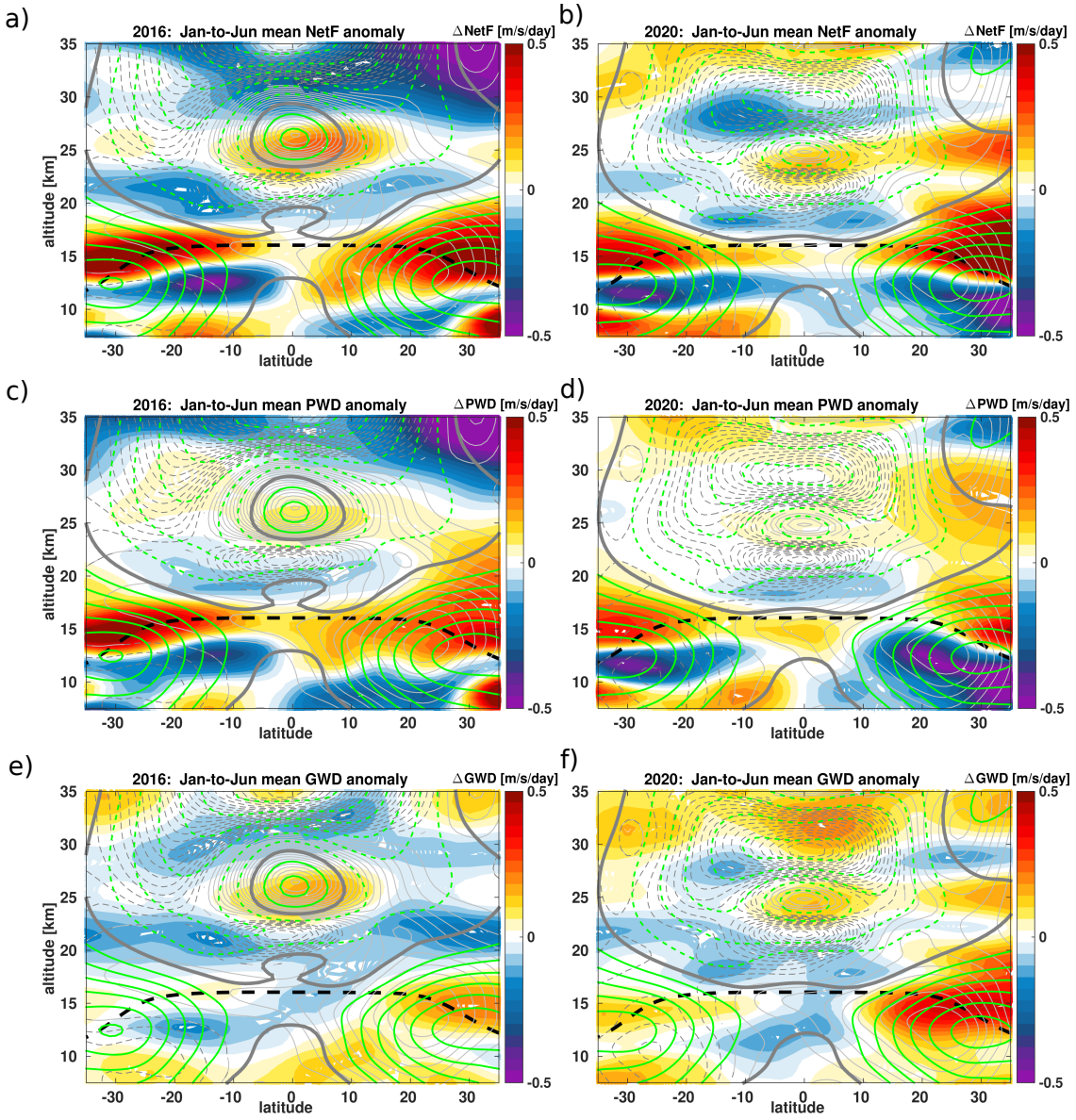

Figure 6. January-to-June 2016 **(a, c, e)** and 2020 **(b, d, f)** deviations from the January–June 1979-to-2014 average of monthly mean zonal mean net wave forcing (NetF) **(a, b)**, planetary wave drag (PWD) **(c, d)** and gravity wave drag (GWD) **(e, f)** from the ERA5 reanalysis (filled contours) together with the January-to-June 2016 and 2020 zonal mean zonal wind (green contours lines) as a function of latitude and altitude. The black dashed horizontal line indicates the tropopause from the ERA5 reanalysis. January-to-June 2016 and 2020 monthly mean zonal mean wind anomaly component, U ($\mathrm{m\,s^{-1}}$), from the ERA5 reanalysis is overlaid as solid grey contours (westerly) and dashed grey contours (easterly) lines.

the good agreement in the structure of planetary and gravity wave breaking, our analyses also show differences in wave drag between the 2016 and 2020 QBO disruption events. The planetary and gravity wave anomalies indicate stronger anomalies in wave dissipation in the lower stratosphere near the equatorward upper flanks of the subtropical jet between the tropopause and the altitude of about 23 km during the QBO disruption event in 2016 than during the QBO disruption event in 2020 (Fig. 6c–f and Fig. S3b, c in the supplement). The anomalies in planetary wave dissipation associated with the QBO disruption event in 2016 are stronger and extend from the tropics toward the subtropical jet between the tropopause and the altitude of about 23 km, while for the QBO disruption event in 2020, these anomalies are smaller and confined to the tropics. In addition to structural differences, the dissimilarities in the strength and depth of the anomalies are even larger in the gravity wave drag. During the QBO disruption event in 2016, gravity waves break in the entire lower stratosphere between the tropopause and the altitude of about 23 km with a maximum occurring near the upper flank of the subtropical jet, a key region for strengthening the shallow branch of the BDC (**???**) (Fig. 6e, f). The differences in the strength and depth of planetary and gravity wave breaking are clearly the main cause of observed differences in the anomalous upwelling strength of the BDC between the year 2016 and the year 2020. This main cause is a combination of planetary wave dissipation in the tropics and particularly strong gravity wave breaking near the equatorward upper flanks of the subtropical jet during the QBO disruption event 2016 as shown in previous studies (**???**). In summary, the strong planetary waves and gravity wave forcing anomalies, which are likely related to ENSO and IOD, are responsible for differences in the anomalous circulation and its modulation by the QBO–induced secondary circulation, therefore, the negative lower stratospheric H_2O and O_3 anomalies. Regardless of the net wave forcing in 2020, the Australian wildfire led to weaker dehydration in the lower stratospheric dehydration due to the aerosol–induced warmer stratosphere.

Note that during the QBO disruption events in 2016 and in 2020, the surface conditions were different in terms of natural variability–induced convective activity. To trace back and link the potential source of convectively generated wave activities to regional differences, we finally analysed the monthly mean Outgoing Longwave Radiation (OLR) (Fig. 7 and Fig. S4 in the supplement). Clearly, there are regional differences in the occurrence of strong convective events between the QBO disruption events in 2016 and 2020. During the QBO disruption event in 2016, the tropical mean OLR anomalies reveal two active convective regions, namely the East Indian Ocean associated with the negative IOD in 2016, and the Central Pacific Ocean associated with the El Niño in the year 2016. However, during the QBO disruption event in 2020, the tropical mean OLR anomalies show only one strong active convective region that is the West Indian Ocean and East Africa associated with the strong IOD in the year 2020 as the weak La Niña is associated to weak tropical convective activities. Both QBO disruption effects related to OLR variations are linked to strong convective activity in the Indo-Pacific Ocean, therefore, suggesting the importance role of this region may play in strong wave activities. This additional information related to the strength of convective activities in the Indian Ocean is of great interest for better understanding and relating the origin of the QBO disruption events and their strength based on regional forcings. This regional forcing and interplay of different modes of climate variability will be presented in further studies.

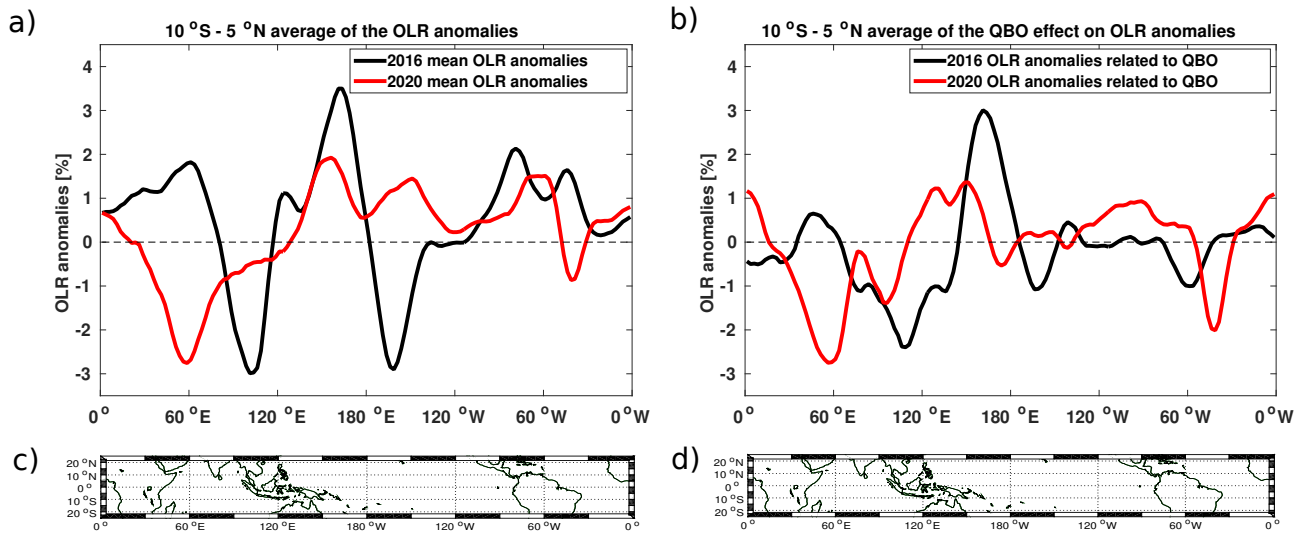

Figure 7. Longitudinal variations of the monthly mean Outgoing Longwave Radiation (OLR) anomalies **(a)** averaged between 20^o S–20^o S together with the 2016 and 2020 QBO effect **(b)** associated with the convective activity derived from the multiple regression fit. The lower-most panels **(c, d)** shows the tropical region where the OLR timeseries are averaged.

5 Summary and conclusions

Based on an established multiple regression method applied to Aura MLS observations, we found that both the QBO disruption events in 2016 and in 2020 induced similar structural changes in the Brewer–Dobson circulation and respective distributions of the lower stratospheric H_2O and O_3 anomalies. Both QBO disruption events induced negative anomalies in H_2O and O_3, a few months after the sudden shift from the QBO westerly to QBO easterly winds ~~reached the tropical tropopause~~. During the boreal winter of 2015–2016 (September 2015–March 2016), the alignment of the strong El Niño and negative IOD events with the QBO westerlies strongly moistened the lower stratosphere between the tropopause and the altitude of 23 km (positive anomalies of more than 20 %). Analogously, the alignment of the weak La Niña and strong positive IOD event with the strong QBO westerlies and the impact of Australian wildfire smoke strongly moistened the lower stratosphere (positive anomalies of more than 15 %) during the boreal winter of 2019–2020 (September 2019–Jun 2020). The sudden shift from the QBO westerly to QBO easterly winds reversed the lower stratospheric moistening, therefore, leading to large negative H_2O and O_3 anomalies of up to about 20 % between 16 km and 23 km by the end of summer 2016 and to small negative H_2O anomalies of up to about 2–3 % and moderate negative O_3 anomalies of up to about 10 % in 2020. These decreases in H_2O and O_3 mixing ratios are due to a strengthening of the tropical upwelling of the BDC, cooling tropical cold–point temperatures and their modulations by the QBO disruption events.

However, differences occur in the strength and depth of the QBO disruption–induced negative H_2O and O_3 anomalies in the lower stratosphere between 2016 and 2020. We found that the impact of the QBO disruption event on lower stratospheric

trace gases is weaker in 2020 than in 2016 up to about 18 % for H_2O anomalies and 10 % for O_3 anomalies between 16 km and 23 km, respectively. The differences in the strength and depth of the O_3 anomalies and its modulation by the QBO disruption events are due to discrepancies in the anomalous tropical upwelling of the BDC, which was up to about 25 % larger in 2016 than in 2020. The analysis of the wave drag shows that the differences in planetary wave breaking in the tropical lower stratosphere between the tropopause and the altitude of about 23 km and the gravity wave breaking near the equatorward upper flanks of the subtropical jet (e.g. region between 10°–30°S/N and above the tropopause level) are the main reasons of the differences in the anomalous tropical upwelling of the BDC and secondary circulation between the year 2016 and the year 2020. The main differences in lower stratospheric H_2O anomalies between the year 2016 and the year 2020 are due to discrepancies in the topical cold–point temperatures induced by the 2020 Australian wildfire smoke. Despite of the anomalous planetary waves and gravity wave activities, which are likely related to ENSO and IOD, the 2020 Australian wildfire predominantly raised~~warmed~~ the cold–point temperatures, therefore, leading to less dehydration of the lower stratosphere.

Finally, our results suggest that the interplay of QBO phases with a combination of ENSO and IOD events, and in particular also wildfires and volcanic eruptions, will be crucial for the control of the lower stratospheric H_2O and O_3 budget in a changing future climate. Especially, when increasing future warming will lead to trends in ENSO (**??**) and IOD (**?**) as projected by climate models, and a related potential increase in wildfire frequency combined with a decreasing lower stratospheric QBO amplitude (**?**) are expected in future climate projections. The interplay will change with strong El Niño/negative IOD and La Niña/strong positive IOD likely controlling the lower stratospheric trace gas distributions and variability more strongly in a future changing climate. Clearly, both ENSO and IOD impact on the tropopause height and tropical cold–point temperatures. Further analysis is needed using climate model sensitivity simulations to pinpoint the impact of these future changes in lower stratospheric trace gases and the related radiative feedback.

Data availability. MLS water vapour and ozone data were obtained from the Goddard Earth Sciences Data and Information Services Center at es Center at doi.10.5067/Aura/MLS/DATA2508 and doi.10.5067/Aura/MLS/DATA2516, respectively. The aerosol optical depth data is available through Khaykin et al. 2020. The ERA5 reanalysis are available at https://apps.ecmwf.int/data-catalogues/era5/?class=ea, last access: 2nd September 2022, through Hersbach et al., 2020.

Author contributions. MD designed the study, conducted research, performed the calculation and the complete analysis of the impact of the QBO disruptions as well as drafted the first manuscript. ME calculated the wave decomposition. FP, MH, ME, JU, SK and MR provided helpful discussions and comments. MD edited the final draft with contributions from all co-authors for communication with the journal.

Competing interests. The authors declare that they have no conflict of interest.

Acknowledgements. Mohamadou Diallo research position is funded by the Deutsche Forschungsgemeinschaft (DFG) individual research grant number DI2618/1-1 and Institute of Energy and Climate Research, Stratosphere (IEK-7), Forschungszentrum in Jülich during which this work had been carried out. FP is funded by the Helmholtz Association under grant number VH-NG-1128 (Helmholtz Young Investigators Group A-SPECi). Manfred Ern was supported by the German Federal Ministry of Education and Research (Bundesministerium für Bildung und Forschung, BMBF) project QUBICC, grant number 01LG1905C, as part of the Role of the Middle Atmosphere in Climate II (ROMIC-II) programme of BMBF. We gratefully acknowledge the Earth System Modelling Project (ESM) for funding this work by providing computing time on the ESM partition of the supercomputer JUWELS at the Jülich Supercomputing Centre (JSC). Moreover, we particularly thank the European Centre for Medium-Range Weather Forecasts for providing the ERA5 and ERA-Interim reanalysis data.